



Solid-State Synthesis, Characterization, Biological studies and Theoretical Evaluation of (E)-2-(2-(naphthalene-2-yloxy)-1-phenylethylidene) Hydrazine thiocarboxamide

G. RAJMOHAN¹, G. RAVINDRAN^{2*} and G. ARIVAZHAGAN^{3**}

¹Department of Physics, Cardamom Planters' Association College, Bodinayakanur, Tamilnadu, India.

²Department of Chemistry, Cardamom Planters' Association College, Bodinayakanur, Tamilnadu, India.

³Department of Physics, Thiagarajar College, Madurai - 625009, Tamilnadu, India.

*Corresponding author E-mail: arivuganesh@gmail.com

<http://dx.doi.org/10.13005/ojc/370312>

(Received: May 20, 2021; Accepted: June 17, 2021)

ABSTRACT

The title compound (E)-2-(2-(naphthalene-2-yloxy)-1-phenylethylidene) hydrazine thiocarboxamide (NAPTCAR) was synthesized by condensing 2-(Naphthalen-2-yloxy)-1-phenylethanone (2-NAPETH) with thiosemicarbazide in 1:1 molar ratio in solid state medium. Purity of compounds has been confirmed by Thin Layer Chromatography. Characterization and structure elucidation of these ligands have been made using ¹H NMR, ¹³C NMR and FTIR spectral studies and DFT calculations. Interestingly, ¹³C NMR spectrum of thiosemicarbazone ligand exhibits the presence of two conformational structures. The HOMO-LUMO energy gap of conformer A is found to be almost equal to that of conformer B. Conformer A is has relatively a stronger nucleophilic character than conformer B as indicated by the molecular electrostatic potential surface. Van der Waals and the steric interactions play a dominant role in stabilizing the structure of both the conformers. The ligands have been examined for antibacterial and antifungal activities and are quite active in this respect.

Keywords: Thiosemicarbazone, Antibacterial, FTIR, NMR, DFT.

INTRODUCTION

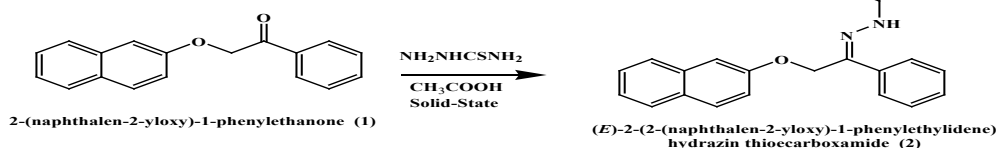
Thiosemicarbazones are imine derivatives obtained by the condensation reaction between aldehydes or ketones and thiosemicarbazide. Different derivatives of thiosemicarbazone can be obtained by suitable substitution. These are versatile intermediates and can be synthesized using simple methods with high yields. Their biological activity is considered to stem from their ability to form chelates with metals. As a class these compounds

are known to exhibit various biological activities like antitumour, antiviral, antibacterial, antiprotozoal and other activities¹⁻³. Their tendency to form Schiff bases with metal cations has attracted the attention of researchers to consider thiosemicarbazones as interesting ligands for synthesizing metal complexes⁴. It is this chelating ability of thiosemicarbazones with endogenous metals that makes them biologically important molecules. Modifications of their structure with different aromatic substituents that can interact with biomolecules enhance their biological activity.



Thiosemicarbazones used to exist in conformational isomeric forms. The stability of the isomeric forms depends on the structural features of the thiosemicarbazone under consideration. Karabatsos *et al.*,⁵⁻⁹ have carried out NMR spectral analysis on aromatic ring substituted phenyl hydrazones, thiosemicarbazones and semicarbazones. The existence of two different isomers of semicarbazones has been reported by Sternberg *et al.*,¹⁰ using proton NMR spectra.

In the present work, the synthesis and characterization of unreported (E)-2-(2-(naphthalene-2-yloxy)-1-phenylethylidene) hydrazine thiocarboxamide (NAPTCAR) using ¹H NMR, ¹³C NMR and FTIR spectral analysis has been presented. The carbon nuclear magnetic resonance spectral data confirm that NAPTCAR exists as two different conformer structures.



Scheme 1. Synthesis of (E)-2-(2-(naphthalene-2-yloxy)-1-phenylethylidene) hydrazine thiocarboxamide(2)

Physical measurements

The uncorrected melting points were found in an open capillary tube. Infra-red spectra of the compounds were recorded using FTIR–Shimadzu model IR-Affinity-1 spectrophotometer using KBr discs in the range 400-4000 cm^{-1} . ¹H NMR and ¹³C NMR spectra have been recorded at 400 and 100 MHz, respectively, using a Bruker Avance III HD Nanobay 400 MHz FT-NMR spectrometer at a temperature of 25°C. CDCl_3 and TMS were used as the solvent and internal standard, respectively.

Antimicrobial examinations

The antifungal and antibacterial activity of thiocarboxamide were allowed to take place in vitro for the growth inhibiting nature against different bacterial and fungal strains utilizing agar disk diffusion method. The cultures were inoculated and incubated for 18 h for the two microorganisms, the nutrient broth and fungi, in potato dextrose agar incline. For the readiness of cultivated agar plate, the liquid medium was poured in sterile petri dish to get a profundity of 5 mm. The medium was allowed to solidify and the test organism was seeded. 5 mL sterile water was added to agar incline culture of organisms to get suspension. A sterile cotton swab

EXPERIMENTAL

Solid-State Synthesis of (E)-2-(2-(naphthalene-2-yloxy)-1-phenylethylidene) hydrazine thiocarboxamide

A mixture of 2-(naphthalene-2-yloxy)-1-phenylethanone (0.1 mol), thiosemicarbazide (0.1 mol) was taken in a test tube. Then the reaction mixture was treated with 5 drops acetic acid and heated at 80°C for about 30 min in water bath. Thin layer chromatography using petroleum ether and ethyl acetate (4:1) as an eluent was used to monitor the progress of the reaction. At the end of the reaction, the reaction mixture was allowed to cool to room temperature. The product was separated, filtered, dried and recrystallized using ethanol. Yield: 86%, Melting range :158-160°C.

was dipped in suspension, daintily spread over the solidified medium. The petri dish was left for a couple of moments. 5 mm whatmann filter paper no.1 discs were dipped in the sample solution. The disc was then removed and placed in a sterile petri dish so that the solvent evaporates. After 10 min the discs were moved to cultivated agar plates. 2 circles were kept on the cultivated agar plate. At last, dishes were incubated at 37°C for bacteria and fungi. Inhibition zones were detected around each disc.

RESULTS AND DISCUSSION

Proton and Carbon NMR Studies

¹H NMR spectrum of (E)-2-(2-(naphthalene-2-yloxy)-1-phenylethylidene) hydrazine thiocarboxamide (NAPTCAR)

In ¹H NMR (400 MHz, CDCl_3), the singlet (Fig. 1) at 5.3 ppm is ascribed to methylene ($-\text{CH}_2-$) group in the product. Another singlet appearing at 10.4 ppm is assigned to the $-\text{NH}$ group. The resonance of the $-\text{NH}_2$ hydrogens gives rise to a broad signal at 6.4 ppm. The remaining phenyl and naphthyl ring protons resonances are given below: 7.20 -7.28 (d, 1H), 7.34-7.46 (m, 6H), 7.67-7.71 (t, 3H), 7.79-7.81 (t, 2H) ppm.

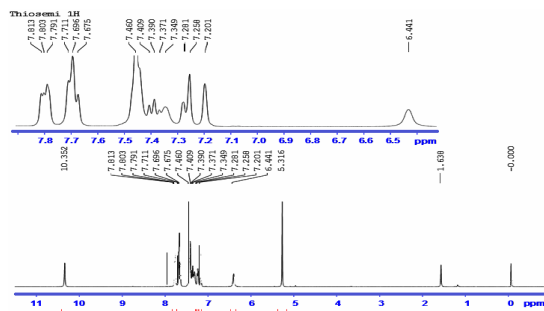


Fig. 1. ^1H NMR spectrum of (E)-2-(2-(naphthalene-2-yloxy)-1-phenylethylidene) hydrazine thiocarboxamide in CDCl_3 at 25°C

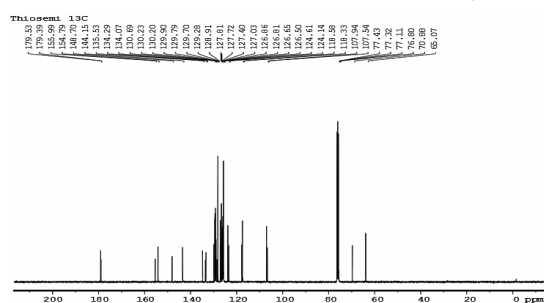
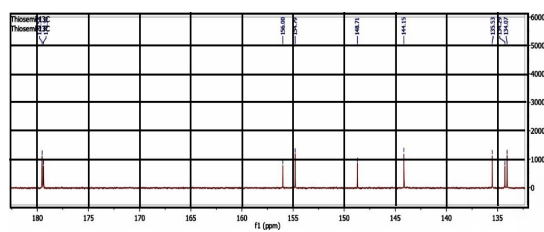
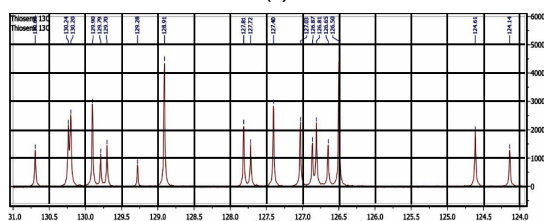


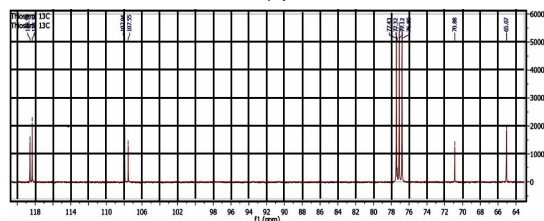
Fig. 2. ^{13}C NMR spectrum of (E)-2-(2-(naphthalene-2-yloxy)-1-phenylethylidene) hydrazine thiocarboxamide in CDCl_3 at 25°C



(a)



(b)



(c)

Fig. 3. Expanded ^{13}C NMR Spectrum of (E)-2-(2-(naphthalene-2-yloxy)-1-phenylethylidene) hydrazine thiocarboxamide in the range of a) 180.0 to 130 ppm, b) 131 to 124 ppm and c) 120 to 64 ppm

^{13}C NMR spectrum of (E)-2-(2-(naphthalene-2-yloxy)-1-phenylethylidene) hydrazine thiocarboxamide (NAPTCAR)

Thiosemicarbazones are well known to exhibit conformational isomerism. The ^{13}C NMR spectrum (Fig. 2) of NAPTCAR displays two sets of carbon resonance peaks indicating the presence of two conformer structures (Fig. 4) which are given below.

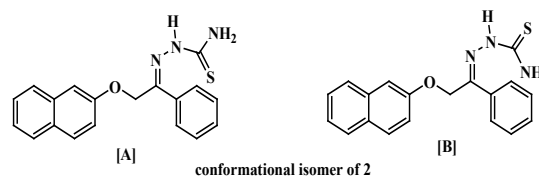


Fig. 4 (A) and (B) are the conformational structures of NAPTCAR

Conformer A The singlet at 65.1 ppm is ascribed to methylene ($-\text{CH}_2$) group in the product. The two singlet signals at 155.9 and 179.3 ppm are assigned to the $-\text{C}=\text{N}-\text{NH}-$ and $-\text{CSNH}_2$ groups, respectively. The remaining phenyl and naphthyl ring carbon peaks are given below: 107.5, 118.3, 124.1, 126.5, 126.8, 127.0, 127.7, 128.9, 129.7, 129.9, 130.2, 134.1, 135.5, 148.7 ppm.

Conformer B The singlet at 70.9 ppm is ascribed to methylene ($-\text{CH}_2$) group in the product. The two singlet signals at 154.7 and 179.5 ppm are assigned to the $-\text{C}=\text{N}-\text{NH}-$ and $-\text{CSNH}_2$ groups, respectively. The remaining phenyl and naphthyl ring carbon absorptions are: 107.9, 118.6, 124.6, 126.7, 126.9, 127.4, 127.8, 129.3, 129.8, 130.2, 130.7, 134.3, 144.2 ppm.

FTIR Spectral analysis

In this present work, the $\nu_s(\text{C}-\text{H})$ has been assigned to the wavenumber higher than the $\nu_{as}(\text{C}-\text{H})$ band position. This is the usual phenomenon that the substituted aromatic compounds¹¹⁻¹⁵ produce the C-H symmetric stretching peaks at higher wavenumbers than the asymmetric vibrational bands. The $\nu_{as}(\text{CH}_2)$ and $\nu_s(\text{CH}_2)$ bands absorb at 2922.2, and 2723.5 cm^{-1} , respectively. The $\nu_{as}(\text{CH}_2)$ and $\nu_s(\text{CH}_2)$ $\nu(\text{C}=\text{N})$ bands are noticed at 2854.7, and 2675.3 cm^{-1} , respectively. All these bands have been shifted to higher wavenumber side in the spectrum (Fig. 5 and Table 1) of NAPTCAR whose formation has been confirmed by the emergence of additional

bands due to the stretching vibrations of NH_2 , N-H, C=N and C=S groups. The $\nu_{\text{as}}(\text{NH}_2)$, $\nu_{\text{s}}(\text{NH}_2)$, $\nu(\text{N-H})$, $\nu(\text{C=N})$ and $\nu(\text{C=S})$ bands are observed at 3444.9, 3342.8, 3568.3, 1606.7 and 684.7 cm^{-1} , respectively. The molecules that have NH_2 group exist usually as the H-bonded networks which can be ascertained from the broad absorption in the region. But, the FTIR spectrum (Fig. 5 and Table 1) of NAPTCAR displays no such spectral feature and this indicates that NAPTCAR molecules do not involve in self-association among themselves.

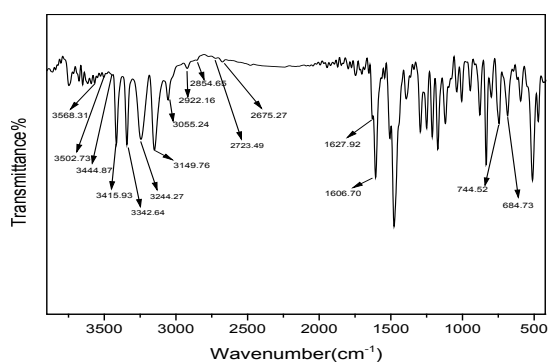


Fig. 5. Experimental vibrational spectrum of NAPTCAR

The theoretical infrared spectra of Conformer A and Conformer B of NAPTCAR are given in Fig. 6 and the assignment of vibrational bands are given in Table 1. The $\nu_{\text{as}}(\text{NH}_2)$, $\nu_{\text{s}}(\text{NH}_2)$, $\nu(\text{N-H})$, $\nu_{\text{s}}(\text{C-H})$, $\nu_{\text{as}}(\text{C-H})$, $\nu_{\text{as}}(\text{CH}_2)$, $\nu_{\text{s}}(\text{CH}_2)$, $\nu(\text{C=N})$ and $\nu(\text{C=S})$ bands are observed at 3704.6, 3571.3, 3610.9, 3211.7, 3181.4, 3119.6, 3068.7, 1610.9 and 744.52 cm^{-1} for conformer A and 3685.15, 3553.51, 3506.78, 3202.06, 3179.79, 3105.38, 2995.57, 1649.65 and 772.23 cm^{-1} for conformer B, respectively. Theoretical FTIR spectra of the compound showed that the results are in agreement with experimental.

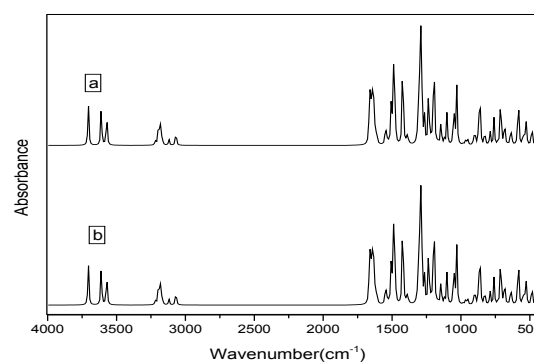


Fig. 6. Theoretical vibrational spectrum of NAPTCAR [(a) Conformer A and (b) Conformer B]

Table 1: Experimental and theoretical vibrational bands (cm^{-1}) of NAPTCAR

Vibrational bands	NAPTCAR			
	Experimental	Theoretical Conformer A	Experimental	Theoretical Conformer B
$\nu_{\text{as}}(\text{NH}_2)$	3444.87	3704.55	3415.93	3685.15
$\nu_{\text{s}}(\text{NH}_2)$	3342.84	3571.34	3244.27	3553.51
$\nu(\text{N-H})$	3568.31	3610.94	3502.73	3506.78
$\nu_{\text{s}}(\text{C-H})$	3149.76	3211.73	3055.24	3202.06
$\nu_{\text{as}}(\text{C-H})$	----	3181.40	----	3179.79
$\nu_{\text{as}}(\text{CH}_2)$	2922.16	3119.56	2854.65	3105.38
$\nu_{\text{s}}(\text{CH}_2)$	2723.49	3068.73	2675.27	2995.57
$\nu(\text{C=N})$	1606.70	1610.85	1627.92	1649.65
$\nu(\text{C=S})$	684.73	749.314	744.52	772.23

Molecular geometry

The structures of the two conformers of NAPTCAR molecule have been optimized at

$\text{B}_3\text{LYP}^{16-17}$ functional of Density Functional Theory (DFT) with the basis set 6-311++G(2d, 2p) using Gaussian 09W program¹⁸ are shown in Figure 7.

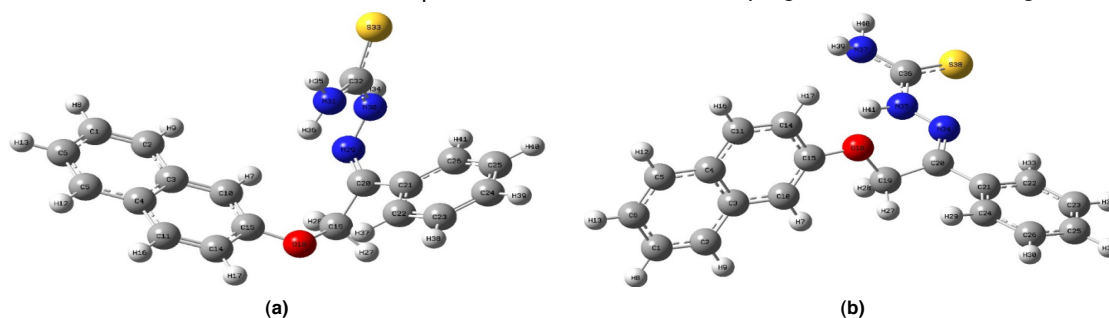


Fig. 7. Ground state optimized structures of NAPTCAR a) Conformer a and b) Conformer b

Frontier molecular orbital (FMO) studies

The frontier molecular orbital examination affords clear ideas about the spatial distribution of the electron density throughout the molecular framework¹⁹⁻²⁰. The energy difference between the highest occupied molecular orbital (HOMO) and lowest unoccupied molecular orbital (LUMO) of a molecule is known as the HOMO-LUMO gap. Using the HOMO-LUMO gap, electrical transport properties²¹ and hence the reactive nature of the conjugated system²² can be explored. The conjugated molecules with a smaller HOMO-LUMO gap are very good candidates for nonlinear optical applications²³⁻²⁴. The HOMO and LUMO diagram of NAPTCAR conformers A and B are shown in Fig. 8. The HOMO which is the electron rich part of the molecule is found to be spread over the carbothioamide group. The LUMO is mainly distributed in the phenyl ring. This is common for both the conformers of NATPCAR. But unlike in conformer A, the LUMO on carbothioamide is a bit more in conformer B. The HOMO-LUMO energy for conformer A is $(-0.2141 - (-0.0788)) = 0.13$ eV which is almost the same that for conformer B $-0.2098 - (-0.0691) = 0.14$ eV. The lower energy gap means that the molecules are more reactive because of the possibility for the easy transition of the electrons from ground state to the excited state.

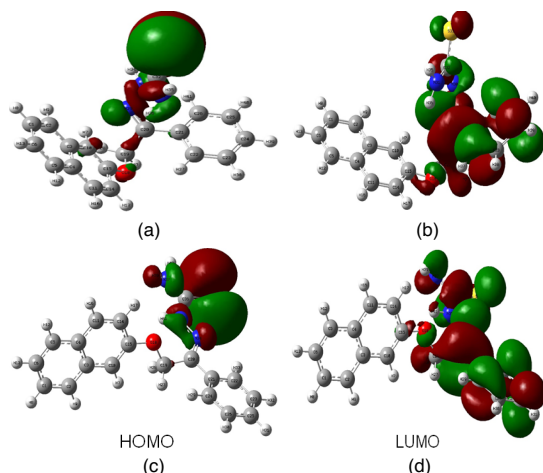


Fig. 8. The HOMO (a and c) of Conformer A and Conformer B form of NAPTCAR and LUMO of Conformer A and Conformer B form (b and d)

Molecular electrostatic potential

The molecular electrostatic potential

(MEP) can be used to obtain information on the electrophilic and nucleophilic sites and hydrogen bonding interactions²⁵⁻²⁸. Fig. 9 shows the MEP of NAPTCAR conformer A and B from which it can be noticed that the electron density is rich over the region (red) around C=S of conformer A while the region around the C=S of conformer B loses the electron density much. At the same time, the electron deficient region (blue) in both the conformers is around the NH₂ hydrogens. Therefore, conformer A has a stronger nucleophilic site, the C=S, than conformer B. But both the conformers are equally good as far as the electrophilic site (blue region) is concerned.

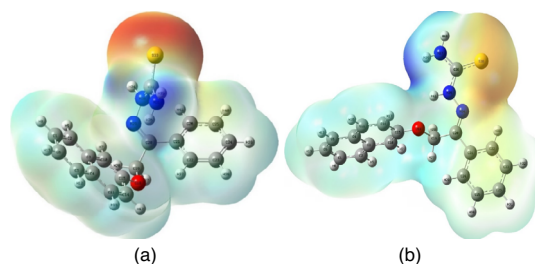


Fig. 9. Electrostatic potential (ESP) surface of (a and b) Conformer A and Conformer B form of NAPTCAR

Reduced density gradient

The RDG isosurface, which can display the presence of various interactions at different parts of the molecule, has been given in Fig. 10. The different types of interactions are indicated by various colours. The presence of strong steric interactions (strong red region) within the phenyl rings in both the conformers can be observed. Van der Waals interactions (green and brown) are found to be operative in conformer A (Fig. 10a) between i) C=N nitrogen and one of the C-H hydrogens of naphthyl ring adjacent to the C-O-C oxygen, ii) CH₂ carbon and one of the C-H hydrogens of the phenyl ring and iii) NH₂ hydrogen and C=N carbon. In conformer B (Fig. 10b), the second interaction continues to be present while new Van der Waals interactions between i) CH₂ carbon and one of the C-H hydrogens of the naphthyl ring, ii) C=N nitrogen and one of the hydrogens of the phenyl ring, iii) C=S sulphur and C=N nitrogen, and iv) notably, a very weak intramolecular H-bond (pale blue) between N-H hydrogen and C-O-C oxygen and steric interaction

(pale red) between N-H nitrogen and C-O-C oxygen are operative. Therefore, it can be stated that conformer B is stabilized by more interaction forces than conformer A.

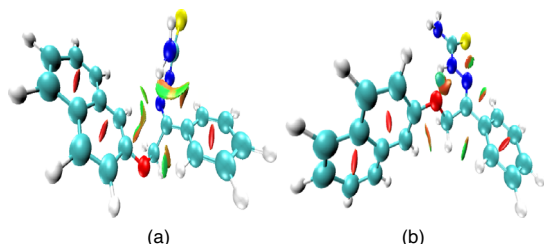


Fig. 10. The reduced density gradient (RDG) isosurfaces of a) conformer A and b) conformer B of NAPTCAR

Table 2: Antimicrobial activities of NAPTCAR

Gram-positive Bacteria	Zone of Inhibition in mm	
	NAPTCAR	Control (Amikacin)
1 <i>Bacillus subtilis</i>	13	26
2 <i>Bacillus cereus</i>	11	26
3 <i>Enterococcus</i>	13	22
4 <i>Staphylococcus aureus</i>	8	27
Gram-negative Bacteria		
1 <i>E.coli</i>	11	22
2 <i>Klebsiella pneumoniae</i>	12	20
3 <i>Pseudomonas aeruginosa</i>	10	27
4 <i>Serratia marcescens</i>	13	25
Fungai		
		Control (Nystatin)
1 <i>Candida albicans</i>	15	18
2 <i>Aspergillus niger</i>	8	12

Antimicrobial activity

The antimicrobial properties of NAPTCAR were evaluated against *Gram-negative* bacterial strains (*Escherichia coli*, *Klebsiella pneumoniae*, *Pseudomonas aeruginosa*, *Serratia marcescens*), *Gram-positive* bacterial strains (*Bacillus cereus*, *Bacillus subtilis*, *Enterococcus*, *Staphylococcus aureus*) and Fungal Species (*Candida albicans*, *Aspergillus niger*). The antimicrobial activity of test compound are expressed as the area of zone of inhibition and summarized in Table 2. The results of antimicrobial screening, Compound

semi exhibited good activity against *Pseudomonas aeruginosa*, *Serratia marcescens*, *Bacillus cereus* and *Enterococcus*. This compound was inactive against fungal species. The thio-semi compound was tested against ten pathogens and active against *Klebsiella pneumoniae*, *Serratia marcescens*, *Bacillus cereus*, and *Enterococcus* and *Candida albicans*. The results of NAPTCAR against pathogenic bacteria and fungi indicate that these may be used for the development of new drugs that can be used to treat microbial infections.

CONCLUSION

The synthesis of (E)-2-(2-(naphthalene-2-yloxy)-1-phenylethylidene) hydrazine thiocarboxamide by simple condensation method and its characterization using NMR (^1H and ^{13}C), FTIR and DFT calculations. Two conformers of NAPTCAR have been identified using ^{13}C NMR spectral data. The HOMO-LUMO energy gap is found to be almost the same for both the conformers. The molecular electrostatic potential surface shows that Conformer A is relatively a stronger nucleophilic than conformer B. The structure of both the conformers are stabilized by mostly Van der Waals and the steric interactions. As suggested by the results of NAPTCAR against pathogenic bacteria and fungi indicate, both the conformers may be used for the development of new drugs that can be used to treat microbial infections.

ACKNOWLEDGMENT

This research did not receive any specific grant from funding agencies in the public, commercial, or not-for-profit sectors.

Conflict of interest

The author declare that we have no conflict of interest.

REFERENCES

1. Tenorio, R.P.; Goes, A.J.S.; Lima, J.G.; Faria, A.R.; Alves, A. J.; Aquino, M.; *Quimica Nova.*, **2005**, *28*, 1030.
2. Beraldo, H., Gambino, D.; *Mini-Rev. Med. Chem.*, **2004**, *4*, 31.
3. Yu, Y.; Kalinowski, D.S.; Kovacevic, Z.; Siafakas, A.; Jansson, P.J.; Stefani, C.; Lovejoy, D.B.; Sharpe, P.C.; Bernhardt, P.V.; Richardson, D.R. *J. Med. Chem.*, **2009**, *52*, 5271.
4. Mirta, R.; Ivica, D.; Marina, C.; Dubravka, M.; *Acta. Crys.*, **2008**, *C64*, 0570.
5. Karabatsos, G. J.; Graham, J.D.; Vane, F.M.; *J. Am. Chem. Soc.*, **1962**, *84*, 753.
6. Karabatsos, G.J.; Shapiro, B.L.; Vane, F.M.; Fleming, J.S.; Ratka, J.S.; *J. Am. Chem. Soc.*, **1963**, *85*, 2784.

7. Karabatsos, G.J.; Taller, R.A.; Vane, F.M.; *J. Am. Chem. Soc.*, **1963**, *85*, 2326.
8. Karabatsos, G.J.; Taller, R.A.; *J. Am. Chem. Soc.*, **1963**, *85*, 3624.
9. Karabatsos, G.J.; Vane, F.M.; Taller, R.A.; His, N.; *J. Amer. Chem. Soc.*, **1964**, *86*, 3351.
10. Stenberg, V.I.; Barks, P.A.; Bays, D.; Hammargren, D.D.; Rao, D.V.; *J. Org. Chem.*, **1968**, *33*, 4402.
11. Stuart, B.H. *Infrared Spectroscopy: Fundamentals and Applications*, John Wiley and Sons, Chichester, **2004**, UK.
12. Wang, Y.; Zhang, Y.; Ni, H.; Meng, N.; Ma, K.; Zhao, J.; Zhu, D.; *Spectrochim. Acta., Part A* **2015**, *135*, 296.
13. Snyder, R.G.; Strauss, H.L.; Elliger, C.A.; *J. Phys. Chem.*, **1982**, *86*, 5145.
14. Lao, W.; Xu, C.; Ji, S.; You, J.; Ou, Q.; *Spectrochim. Acta, Part A.*, **2000**, *56*, 2049.
15. Palafox, M.A.; *Int. J. Quantum Chem.*, **2000**, *77*, 661.
16. Becke, A. D.; *J. Chem. Phys.*, **1993**, *98*, 5648.
17. Lee, C.; Yang, W.; Parr, R. G.; *Phys. Rev., B* **1988**, *37*, 785.
18. M. J. Frisch.; G. W. Trucks.; H. B. Schlegel.; G. E. Scuseria.; M. A. Robb.; J. R. Cheeseman.; G. Scalmani.; V. Barone.; B. Mennucci.; G. A. Petersson.; H. Nakatsuji.; M. Caricato.; X. Li, H. P. Hratchian.; A. F. Izmaylov.; J. Bloino.; G. Zheng.; J. L. Sonnenberg.; M. Hada.; M. Ehara.; K. Toyota.; R. Fukuda.; J. Hasegawa.; M. Ishida.; T. Nakajima.; Y. Honda.; O. Kitao.; H. Nakai.; T. Vreven.; J. A. Montgomery, Jr., J. E. Peralta.; F. Ogliaro.; M. Bearpark.; J. J. Heyd.; E. Brothers.; K. N. Kudin.; V. N. Staroverov.; T. Keith.; R. Kobayashi.; J. Normand.; K. Raghavachari.; A. Rendell.; J. C. Burant.; S. S. Iyengar.; J. Tomasi, M. Cossi, N. Rega.; J. M. Millam.; M. Klene.; J. E. Knox.; J. B. Cross.; V. Bakken.; C. Adamo.; J. Jaramillo.; R. Gomperts.; R. E. Stratmann.; O. Yazyev.; A. J. Austin.; R. Cammi.; C. Pomelli, J. W. Ochterski.; R. L. Martin.; K. Morokuma.; V. G. Zakrzewski.; G. A. Voth.; P. Salvador, J. J. Dannenberg.; S. Dapprich.; A. D. Daniels.; O. Farkas.; J. B. Foresman.; J. V. Ortiz.; J. Cioslowski and D. J. Fox.; Gaussian 09.; Revision D.01, Gaussian, Inc., Wallingford CT., **2010**.
19. Latha, V.; Annaraj, B.; Neelakantan, M.A.; *Spectrochim. Acta Part A.*, **2014**, *133*, 44.
20. Fukui, K. *Angew. Chemie Int. Ed. English.*, **1982**, *21*, 155.
21. Fukui, K. *Science.*, **1982**, *218*, 747.
22. Fukui, K.; Yonezawa, T.; Shingu, H.; *Chem. J. Phys.*, **1952**, *20*, 722.
23. Choi, C.H.; Kertesz, M.; *Chem. J. Phys.*, **1997**, *101A*, 3823.
24. Kurt, M.; Chinnababu, P.; Sundaraganesan, N.; Cinar, M.; Karabacak, M.; *Spectrochim. Acta A.*, **2011**, *79*, 1162.
25. Scrocco, E.; Tomasi, J.; *Topics in Current Chemistry*, **1973**, *7*, Springer, Berlin.
26. Luque, F.J.; Lopez, J.M.; Orozco, M.; *Theor. Chem. Acc.*, **2000**, *103*, 343.
27. Okulik, N.; Jubert, A.H.; *Internet Electronic. J. Mol. Des.*, **2005**, *4*, 17.
28. Pathak, S.K.; Srivastava, R.; Sachan, A.K.; Prasad, O.; Sinha, L.; Asiri, A.M.; Karabacak, M.; *Spectrochim. Acta., A* **2015**, *135*, 283.